Electronic Supplementary Information (ESI): Dendritic silver self-assembly in molten-carbonate membranes for efficient carbon dioxide capture

Liam A. McNeil,[a] Greg A. Mutch,[a] Francesco Iacoviello,[b] Josh J. Bailey,[b] Georgios Triantafyllou,[a] Dragos Neagu,[a] Thomas S. Miller,[b] Evangelos I. Papaioannou,[a] Wenting Hu,[a] Dan J.L. Brett,[b] Paul R. Shearing[b] and Ian S. Metcalfe[a]

[a] *School of Engineering, Newcastle University, Merz Court, Newcastle upon Tyne NE1 7RU, U.K.*
[b] *Electrochemical Innovation Lab, Department of Chemical Engineering, UCL, London WC1E 7JE, U.K.*

Experimental Methods:

Dual-phase pellet membrane preparation

Four types of dual-phase pellet membranes were prepared; an Al_2O_3-supported membrane and three Ag-modified Al_2O_3-supported membranes, the latter prepared using three different Ag incorporation procedures. To prepare the ternary eutectic carbonate mixture for use as the molten carbonate (MC) phase (melting point, $T_m \approx 400$ °C),[1] Li_2CO_3, Na_2CO_3 and K_2CO_3 (Alpha Aesar, ACS, 99.5% min) were dried separately in air at 300 °C for 24 hours, then mixed in a 43.5/31.5/25 mol% ratio.

Porous Al_2O_3 pellet supports were prepared by mixing 1.0 g of α-Al_2O_3 powder (Alpha Aesar, ACS, 99.5% min) with 0.7 ml of 10 wt% polyvinyl alcohol (PVA) binder (powders of PVA 10-98 (Fluka, Mw ~61000) into warm deionised water). The mixture was pressed at 3 tonnes (Atlas Power T25 hydraulic press) to form 1.75 mm thick, 20 mm Ø pellets, which were heated in air to 1200°C at 2°C min^{-1} and sintered at this temperature for 5 hours.

To prepare Ag-modified membranes, three methods were used. First, electroless plating was used to deposit a layer of Ag on the surface of Al_2O_3 pellets, following previously reported methods.[2,3] PTFE tape was used to mask the pellets, leaving a central 14 mm Ø of one of the 20 mm Ø faces exposed. The exposed side was activated with Pd nuclei *via* sensitisation in an acidic $SnCl_2$ solution, followed by activation in an acidic $PdCl_2$ solution, with intermittent rinsing in deionised water or HCl (Fig. S1 and Table S1). The chemical baths were homogenised by air bubbling and the sensitisation/activation process was repeated for six cycles.

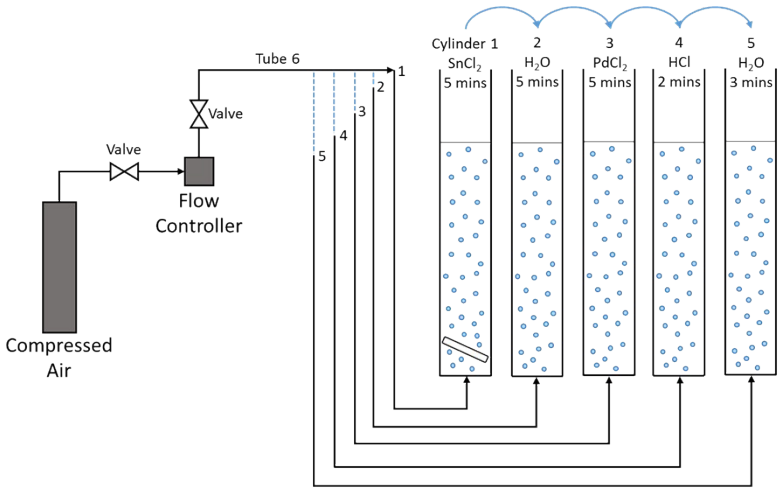

Fig. S1: Sensitisation/activation of Al_2O_3 pellets with Pd nuclei. A series of chemical baths with air bubbling for mixing, and associated procedural timings, to prepare Pd activated pellets for electroless plating with Ag. Solution compositions provided in Table S1.

Table S1: Sensitisation/activation and electroless-plating solutions. Composition of solutions used for membrane preparation processes in Fig. S1 and Fig. S2.

Step	Reagent	Concentration (mol l^{-1})
Sensitisation	$SnCl_2$	4.43×10^{-3}
	HCl	3.29×10^{-2}
Activation	$PdCl_2$	5.64×10^{-4}
	HCl	3.29×10^{-2}
Rinsing	HCl	1.00×10^{-2}
Electroless plating	$AgNO_3$	3.06×10^{-3}
	Na_2EDTA	1.19×10^{-1}
	NH_4OH	4.97
	N_2H_4	1.75×10^{-1}

Electroless plating of a Ag layer was performed by immersing the Pd-activated Al_2O_3 pellets in 18 ml of plating solution, homogenised by air bubbling, at 60 °C for 1 hour (Fig. S2 and Table S1). Pellets were washed in deionised water and re-immersed in fresh plating solution, repeated for six cycles, to gradually replace Pd nuclei with a layer of metallic Ag.

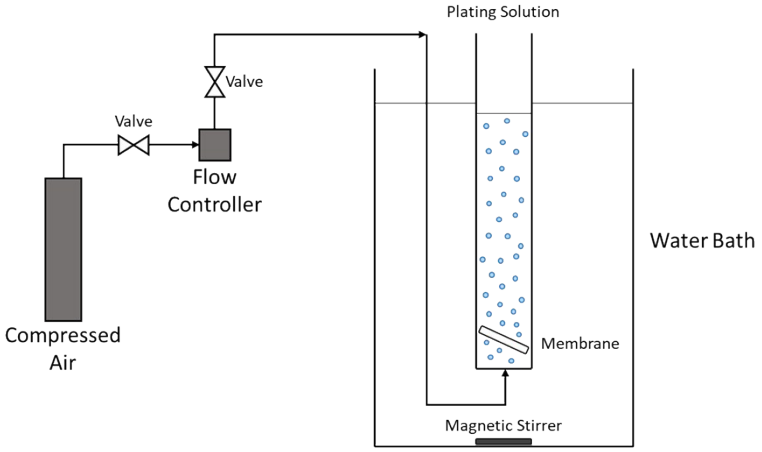

Fig. S2: Electroless plating of Al_2O_3 pellets. Temperature-controlled chemical bath to prepare an electroless-plated layer of Ag on Al_2O_3 pellets. Solution composition given in Table S1.

Second, to deposit well-dispersed nanoscale metallic Ag particles throughout the internal and across the external surfaces of the Al_2O_3 pellets, dry impregnation was used. Based on the porosity of the Al_2O_3 pellet, 0.3 ml of a 1.25×10^{-5} M $AgNO_3$ solution was added dropwise, before drying in air at 100 °C for 12 hours. To decompose $AgNO_3$ and form nanoscale Ag, impregnated pellets were heated in air to 600°C at 1°C min^{-1} and held at this temperature for 3 hours.

Third, Ag was directly loaded into the ternary eutectic carbonate mixture described above. Metallic Ag powder (Alfa Aesar, -100 mesh (<150 µm), 99.95% metals basis) was added to produce Ag mole fractions ranging from 0-10 mol% (on a metal basis).

Parallel-pore membrane

A membrane support with a parallel pore network was manufactured using an Al_2O_3 tube (200 mm length, 20 mm outer Ø, 15 mm inner Ø), closed at one end (closed-end thickness, ~500 µm) (Precision Ceramics) (Fig. S3). The tubular support was laser-drilled at Laser Micromachining Ltd. with 2000 parallel pores in the centre of the closed end covering an area of ~180 mm^2 (~15 mm Ø). The pores were conically shaped (due to the inherent Gaussian shape of the laser beam), and of 75 µm Ø on the permeate side (inside the tube) and 150 µm Ø on the feed side (laser incident surface) (detail provided by Laser Micromachining Ltd.). Ag was introduced to the membrane by doping the ternary eutectic carbonate mixture with Ag powder, described previously.

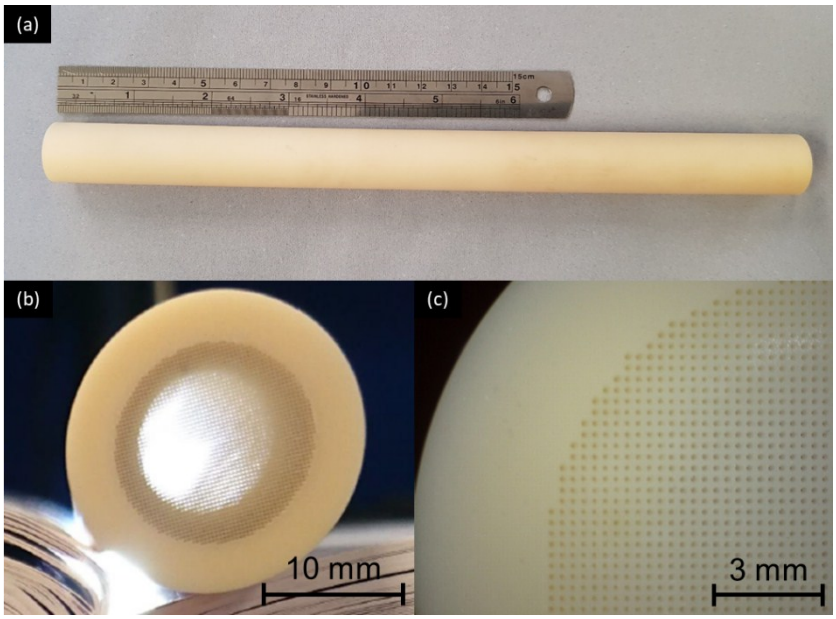

Fig. S3: Tubular parallel-pore Al_2O_3 membrane support. (a) Closed-end Al_2O_3 tube, (b) laser-drilled closed-end and, (c) microscope image of the laser-drilled parallel pores.

Permeation measurements

Pellet membranes were attached to an Al_2O_3 tube (9 mm inner Ø, 12 mm outer Ø) using gold ink (Fuelcellmaterials, 70 wt%) and inserted into a custom-made membrane reactor (Fig. S4). The gold ink was cured to form a gas-tight seal, using the following temperature programme: 1) heating in air from room temperature to 850°C at 1°C min^{-1}; 2) curing at 850°C for 1 hour, and 3) cooling to room temperature at 1°C min^{-1}. It is important to note that the effective permeate-side Ø was 7 mm, as permeated gases were collected from the inside of the Al_2O_3 tube (of the 9 mm inner Ø of the Al_2O_3 tube, 2 mm was lost due to gold sealant spreading during curing). After the reactor was cooled, 0.6 g of the ternary eutectic carbonate mixture (with or without Ag loading) was pressed into a 20 mm Ø pellet, and placed on top of the pellets in the membrane reactor. The amount of carbonates used was calculated to entirely occupy the pore structure of the pellet based on MIP porosity results. The overall porosity $(P\%)$ was found using Equation S1, where ρ_d is the sample bulk density (g/cm^3) and V_i is the volume of sample intruded by mercury (cm^3/g):

$$P\% = \rho_d V_i \times 100 \quad \text{(S1)}$$

The reactor was enclosed using a quartz tube (35 mm outer Ø) and heated to 450 °C at 1°C min^{-1} (*i.e.* above the T_m of the ternary eutectic carbonate mixture). To avoid carbonate decomposition during heating, 50 mol% CO_2, 25 mol% O_2 and 25 mol% N_2 was fed to both feed and permeate sides of the membrane at 30 ml min^{-1} (measured at NTP with calibrated Brooks Smart II mass flow controllers). The same flow rate was used for all gases in all permeation experiments. After holding at 450°C for 1 hour, to allow time for MC to infiltrate the porous pellet supports, the reactor was then heated to 650-750 °C at 1°C min^{-1}, depending on the experiment, whilst maintaining the same gas flow rate and composition on both feed and permeate sides of the membrane. Upon reaching the target temperature, the permeate-side inlet gas was switched to pure Ar, while the feed-side inlet gas remained unchanged. Different inert gases (N_2 on the feed side and Ar on the permeate side) were used to detect transmembrane leaks.

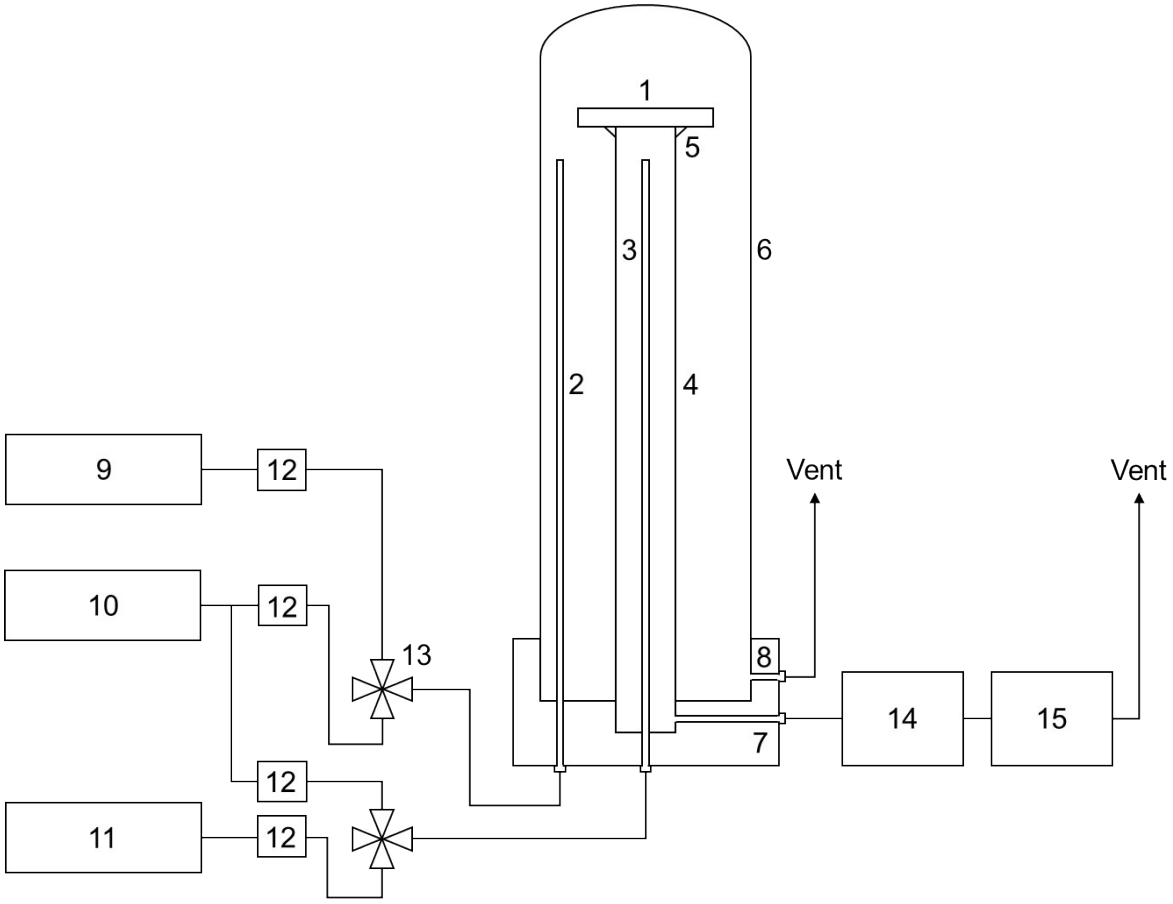

Fig. S4: High temperature membrane reactor and analytical apparatus. (1) Dual-phase membrane, (2) feed-side inlet, (3) permeate-side inlet, (4) Al_2O_3 tube, (5) gold-ink sealant, (6) quartz tube, (7) permeate-side outlet, (8) feed-side outlet, (9) 50% CO_2, 25% O_2 in N_2 gas cylinder, (10) 50% CO_2 in N_2 gas cylinder, (11) Ar gas cylinder, (12) mass flow controllers, (13) 4-way valve, (14) FTIR, and (15) mass spectrometer. In the case of the parallel-pore membrane, (1), (4) and (5) were replaced with the parallel-pore membrane.

During permeation, the permeate-side outlet gas was monitored using two different instruments (Fig. S4). The mole fraction of CO_2 on the permeate side was recorded using an FTIR analyser (MKS MultiGas Analyzer - 2030), with O_2 and N_2 (the latter for leak detection) mole fractions monitored using a mass spectrometer (Hiden Analytical QGA). Experiments were abandoned if the N_2 signal (m/z = 28) exceeded 11% of the CO_2 signal (m/z = 44), after the background had been subtracted. This procedure was adopted as the CO^+ fragment from a pure CO_2 feed gas was 11% of the m/z = 44 channel. If N_2 was permeating, also at m/z = 28, the signal would increase beyond 11% of the m/z = 44 channel. Further transmembrane leak tests were performed during operation, by switching the original feed gas (50 mol% CO_2, 25 mol% O_2 and 25 mol% N_2) to a feed gas containing a higher mole fraction of N_2 (50 mol% CO_2 and 50% N_2). If a leak had occurred during operation, the N_2 signal from the mass spectrometer (m/z = 28) increased, due to the increased driving force for N_2 across the membrane, and the experiment was stopped.

Before and after each permeation experiment, the mass spectrometer and FTIR were calibrated to account for systematic error, instrument drift and air ingress into the apparatus. Calibration was performed by flowing gases (Ar, CO_2, O_2 and N_2) of certificated mole fraction (as close to the expected permeate-side mole fraction during the experiment as possible) through the reactor, FTIR and mass spectrometer. Ar was calibrated first and used to obtain a background for all instruments. CO_2 was calibrated separately from O_2 and N_2 to ensure there was no overlap of m/z = 28 in the mass spectrometer. To assess systematic error in our determination of CO_2 flux a certified 414 ppm CO_2 in N_2 mixture was supplied to the FTIR for 1 hour. Under measurement conditions identical to permeation experiments, an average of 410 ± 1.4 ppm was recorded, indicating a systematic error of < ±1%.

Permeate-side mole fractions of CO_2 and O_2 were converted to flux, permeability and permeance using Equations S2, S3 and S4, respectively, where y_i represents the mole fraction of *i* in the gas phase (here, *i* = CO_2 or O_2), Q_G is the volumetric flow rate of the permeate-side gas (ml min^{-1}), A is the effective permeate-side area (cm^2), $Pa\,i$ and $Pa\,i$ are the partial pressures of CO_2 or O_2 on the feed side and permeate side, respectively (Pa) and l is the membrane thickness (m). CO_2/N_2 selectivity was calculated using the limit of detection for N_2 (10 ppm) in the mass spectrometer (as above, if N_2 was detected, experiments were stopped, so the only available route for calculating selectivity is to assume N_2 present at the limit of detection, which is an inherently conservative approach).

Flux (ml min^{-1} cm^{-2}):

$$J_i = \frac{y_i \times Q_G}{A} \tag{S2}$$

Permeability (mol m^{-1} s^{-1} Pa^{-1}):

$$Permeability = \frac{y_i}{60 \times 22400} \times \frac{1}{A \times 10^{-4}} \times \frac{1}{Pa''_i - Pa'_i} \times l \tag{S3}$$

Permeance (mol m^{-2} s^{-1} Pa^{-1}):

$$Permeance = \frac{Permeability}{l} \tag{S4}$$

The effective permeate-side area for pellet membranes was defined by the 7 mm Ø support tube, and was 0.38 cm^2. The effective permeate-side area for parallel-pore membranes was defined as the sum of the areas of the 75 µm Ø pores on the internal surface of the tubular support, and was 0.088 cm^2. To calculate permeability normalised for quantity of Ag and membrane volume, for our membranes and Ag membranes in the literature, the active volume of membrane was first determined. In the case of cylindrical pellet membranes, the active area for permeation was defined as above (by support tube sealing geometry, commonly reported in dual-phase membrane literature) and multiplied by membrane thickness to arrive at a cylindrical active membrane volume. To calculate the quantity of Ag in pellet membranes in the literature, the active volume of the membrane was multiplied by ρ_{Ag}, with the porosity of the pellet accounted for, and subsequently converted to moles of Ag. For our parallel-pore membrane the sum of the volumes of the 2000 truncated conical pores was taken as the active volume. For our pellet and parallel-pore membranes, the quantity of Ag added during preparation was converted to moles of Ag.

Dual-phase membrane characterisation

For *ex-situ* characterisation of membranes during permeation, quenching of membranes was performed by rapid cooling under permeating conditions.

Microstructural and compositional analysis was performed using scanning electron microscopy (Hitachi TM3030SEM), under an accelerating voltage of 15 kV and with a working distance of 8 mm, equipped with energy dispersive X-ray spectroscopy (Bruker Quantax 70 EDX). Cross-sectional analysis was performed by supporting pellets in epoxy resin (EpoFix, Struers) before cutting, and polishing with silicon carbide papers and a series of diamond pastes, down to 1 μm, before gold-coating. Pellets prepared using dry impregnation were analysed after gold-coating using a Tescan Vega 3LMU, under an accelerating voltage of 8 kV and with a working distance of 8 mm.

Phase identification was completed using X-ray diffraction (XRD, PANalytical X'Pert Pro MPD with CuK_α radiation), powered by a Philips PW3040/60 X-ray generator operating at 40 kV and with a current of 40 mA, and fitted with an X'Celerator detector. Pellets were mounted onto a stainless steel sample holder. Diffraction data was collected over the range of 10-100° 2θ with a step size of 0.03°, and nominal counting time per step of 500 s. A Ni-filter was used in the diffracted beam path to eliminate K_β peaks. Fixed divergence and anti-scatter slits of 1/4° and 1/4°, respectively, were used together with a beam mask of 10 mm and soller slits of 0.04 radians. Phase identification was carried out using PANalytical HighScore Plus in conjunction with the International Centre for Diffraction Data (ICDD) Powder Diffraction File 2 Database (2004).

The pellets' pore size distribution was characterised using mercury intrusion porosimetry (MIP, Pascal 440 Porosimeter) over a pressure range of 0.01-1000 MPa (indicating a pore-size cut-off of ~5 nm) and with a set stabilisation time of 10 s.

X-ray micro-computed tomography (micro-CT) was performed using a Zeiss Xradia 520 Versa (Carl Zeiss X-ray Microscopy, Pleasanton, USA) and a Nikon XT H 225 (Nikon Metrology UK Ltd, Tring, UK). The scan performed on the Zeiss Xradia 520 Versa was conducted at an optical magnification of 4x, which combined with geometrical magnification and binning 1 gave a voxel dimension of 0.897 μm, at a voltage and power of 80 kV and 7W, respectively. The exposure time used for this scan was 15 s, to give average counts above 5000 and the number of projections was 2201. The series of scans performed on the Nikon XT H 225 were all conducted at a voxel dimension of 10.5 μm, at voltage and current of 160 kV and 50 μA, respectively. The exposure time used for each scan was 1 s and the number of projections for each scan was 3176, as per manufacturer default settings. High grayscale Ag voxels were segmented from the lower grayscale Al_2O_3 voxels by a mixture of simple thresholding and manual tweaking, to ensure bright imaging artefacts did not give an erroneous over-allocation of silver. Volume calculations were conducted by simple voxel counting, and multiplication by the cube of the voxel dimensions (10.4 um^3).

The electrical conductivity of membranes was derived from four-point DC resistance measurements. For each measurement a thin Ag electrode was deposited on both the feed side and permeate side of the membranes, to serve as current collectors. The measured voltage was adjusted in the range of 50-500 mV and the corresponding current was measured and recorded across the probes connected to the Ag electrodes.

Supplementary Data:

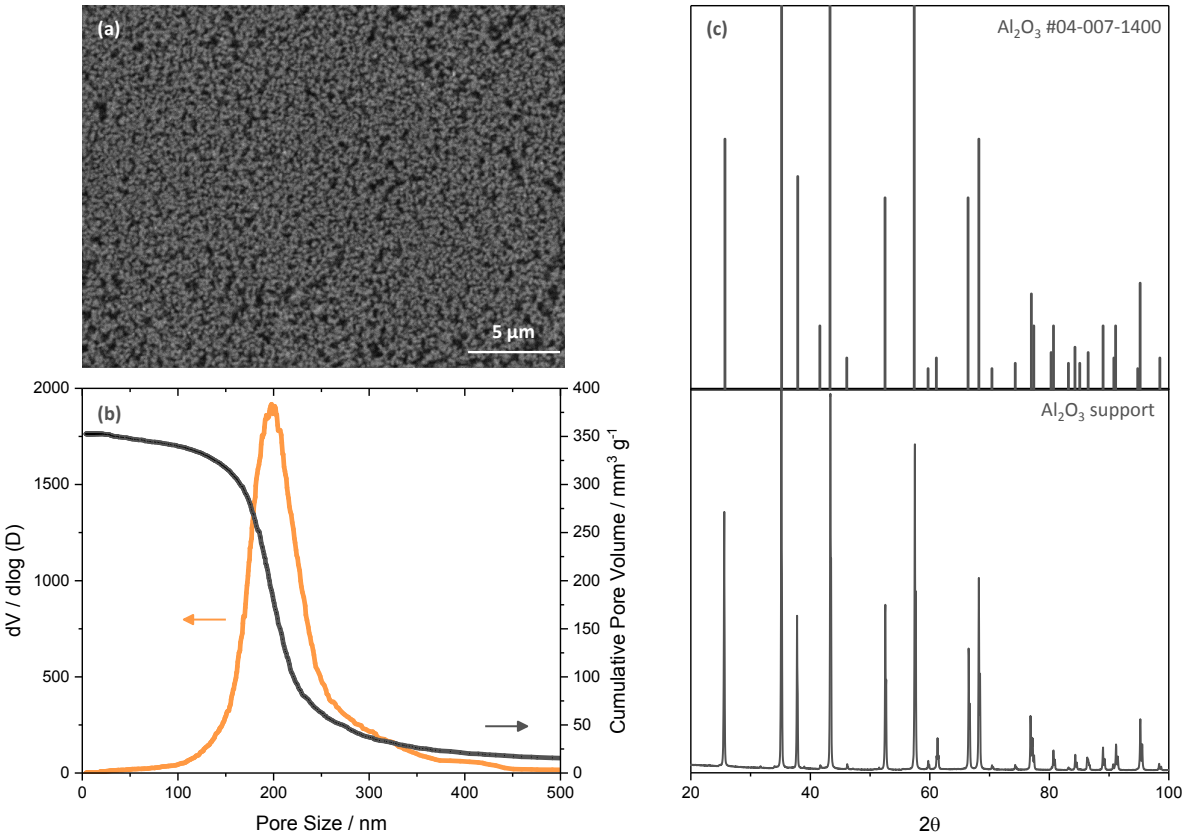

Fig. S5: Microstructure and phase identity of Al_2O_3 pellet membrane supports. (a) SEM image of the pellet surface following controlled sintering, (b) pore size distribution and cumulative pore volume determined by MIP, and (c) phase identification of the support using X-ray diffraction and the ICDD database.

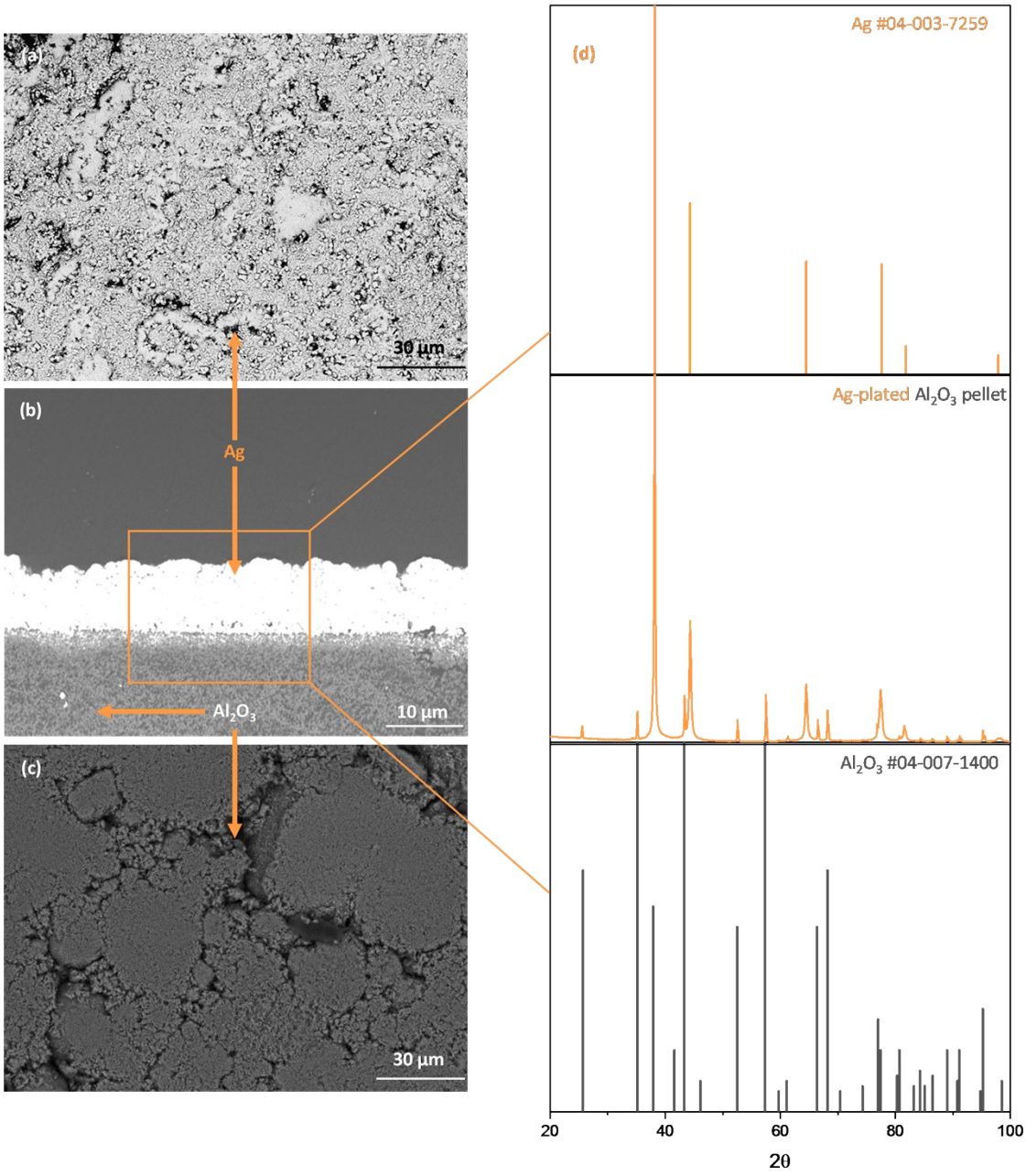

Fig. S6: Microstructure and phase identity of Ag-plated Al_2O_3 membrane supports. SEM images of (a) feed side, (b) cross-section, (c) permeate side and (d) phase identification of the plated supports using X-ray diffraction and the ICDD database.

Calculation of the volume of Ag from SEM images, assumed the Ag-plated area was cylindrical and used Equation S5, where V_{Ag}, Ø and h are the volume (cm^3), diameter (cm) and thickness (cm) of the plated Ag layer, respectively. The mass of the Ag-plated layer (m_{Ag}) was calculated from the volume and the density of Ag (ρ_{Ag}) using Equation S6.

$$V_{Ag} = \frac{\pi Ø^2}{4} h \tag{S5}$$

$$m_{Ag} = V_{Ag} \times \rho_{Ag} \tag{S6}$$

For the pellet used in the permeation experiment (Fig. S7), the mass determined from SEM was 17 mg. Gravimetric analysis of a number of pellets used during the investigation gave an average (n = 10) deposited Ag mass of 17.0 ± 0.3 mg, demonstrating that the porosity of the Ag layer had a negligible impact on determination of Ag mass from SEM images.

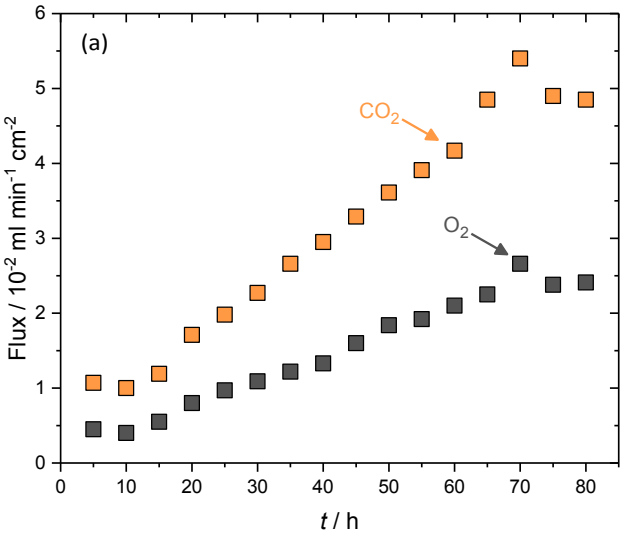

(b)

Fig. S7: CO_2 and O_2 flux evolution at 650°C in Ag-plated and unmodified, dual-phase Al_2O_3 membranes. (a) Electroless-plated Ag pellet membrane, and (b) Al_2O_3 supported pellet membrane. Feed-side inlet: 50 mol% CO_2, 25 mol% O_2 and 25 mol% N_2. Permeate-side inlet: Ar.

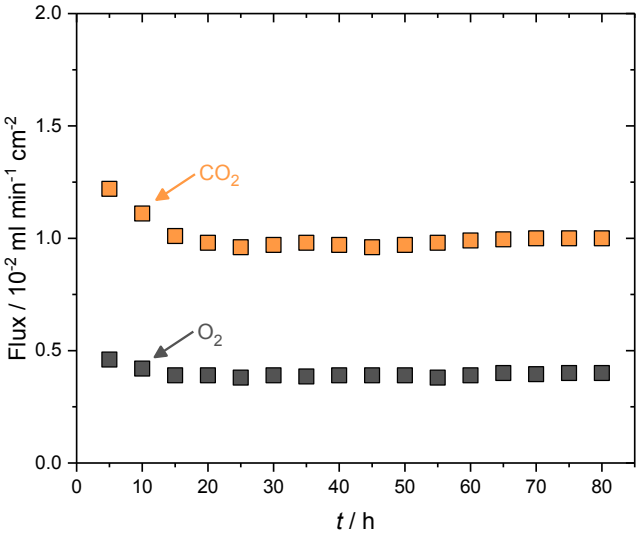
2.0
1.5
1.0
0.5
0.0
Flux / 10-2 ml min-1 cm-2
CO2
O2
0
10
20
30
40
50
60
70
80
t / h

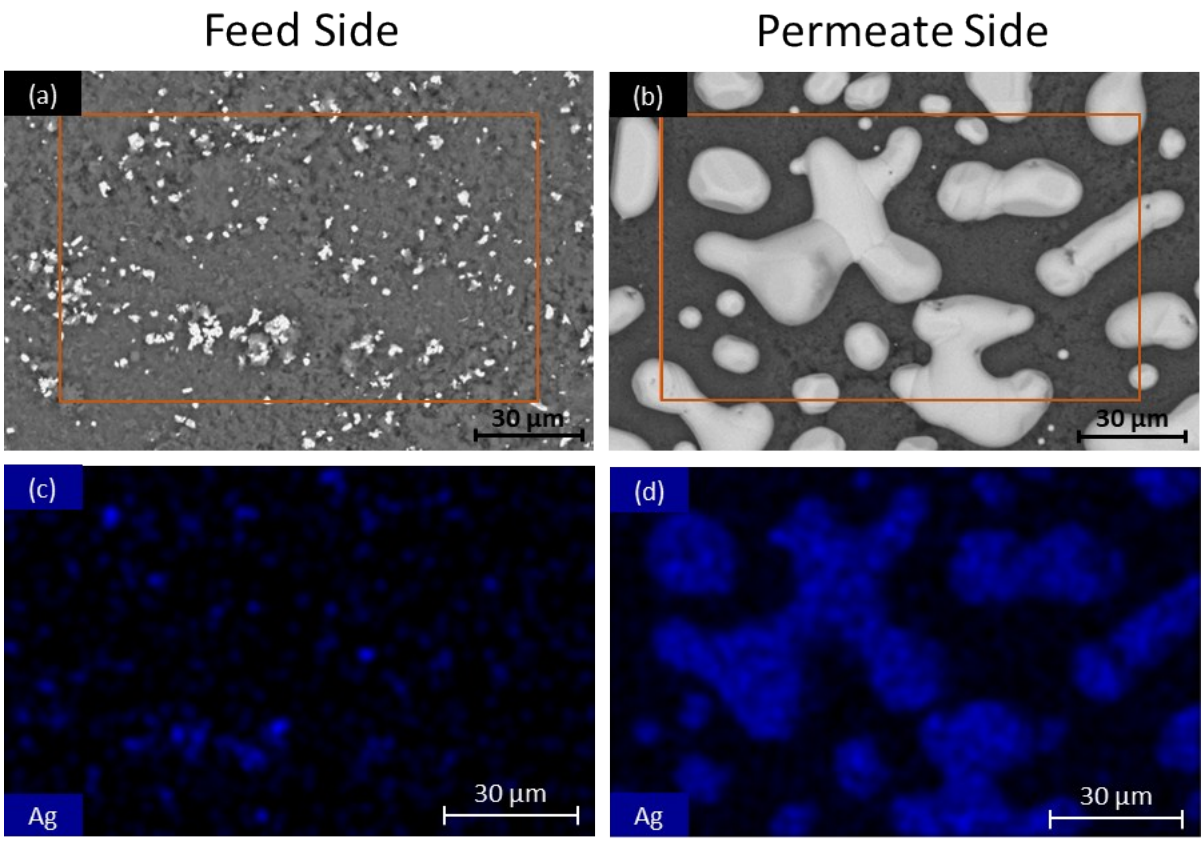

Fig. S8: Ag migration from feed to permeate side after permeation experiment in Fig. S7. (a), (b) SEM images of the feed and permeate side demonstrating dissolution of Ag on the feed-side surface and migration to the permeate-side surface, (c), (d) EDX mapping of Ag from the areas defined by the red boxes in (a) and (b), respectively.

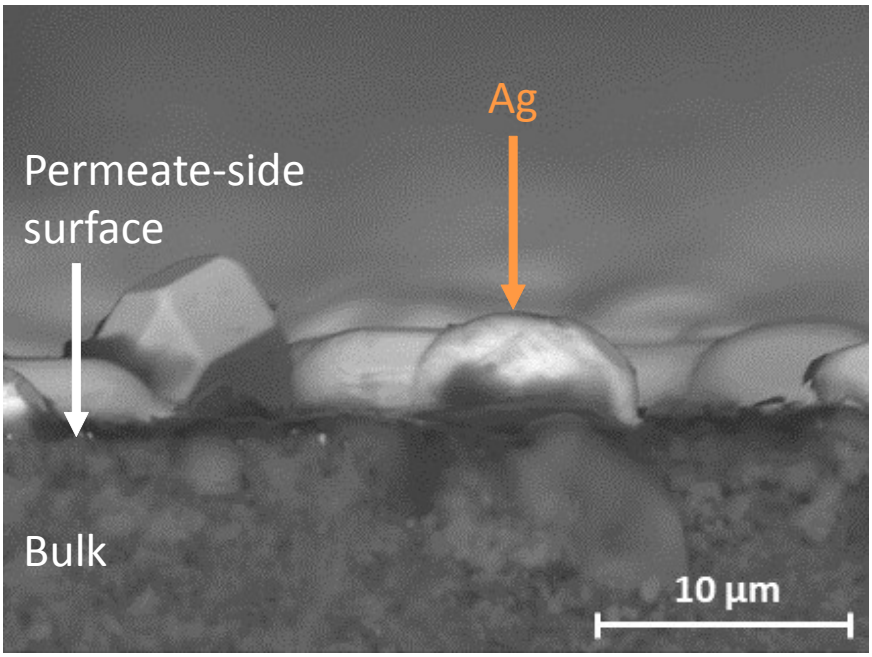

Fig. S9: Migrated Ag after permeation experiment in Fig. S7. Cross-section SEM image of the permeate-side surface.

Calculation of the mass of Ag that migrated to the permeate side following permeation used Equations S5 and S6, where V_{Ag} was determined by surface are mapping of Ag particles on the permeate side using ImageJ, combined with permeate-side cross-section SEM images (Fig. S9) used to determine average Ag particle thickness.

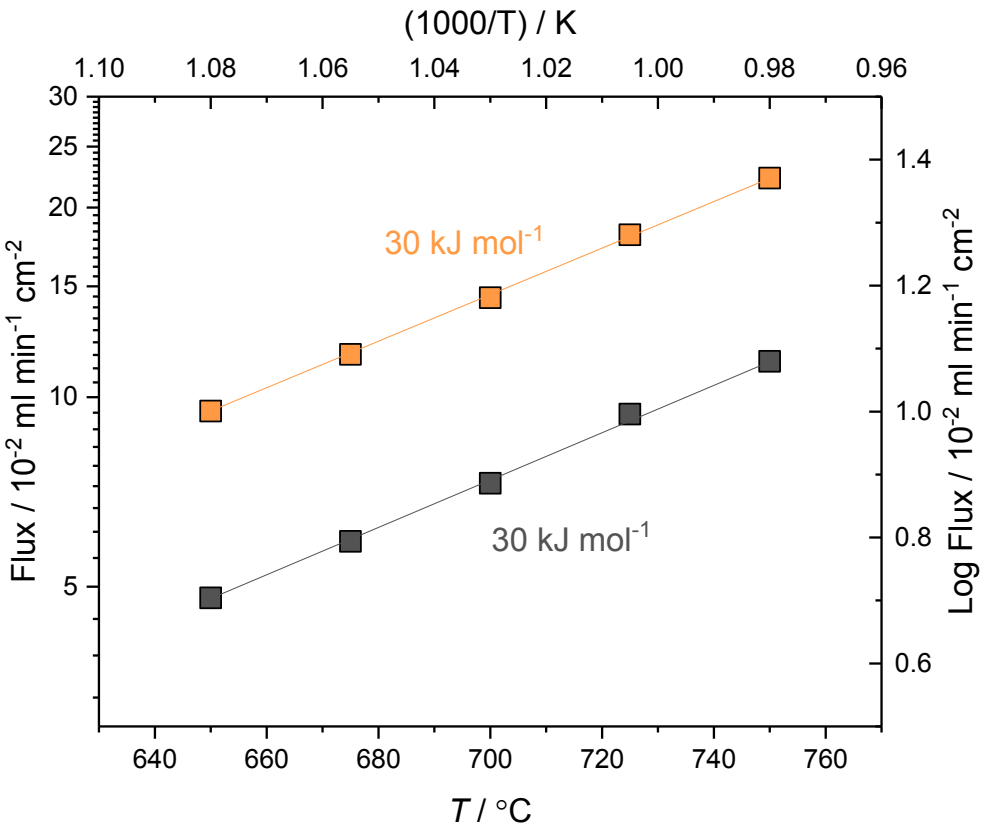

Fig. S10: Arrhenius plot of stable CO_2 and O_2 fluxes in Ag-loaded membranes with 6 mol% Ag loading. Permeation experiments were conducted until stable fluxes were achieved at 650-750 °C. Feed-side inlet: 50 mol% CO_2, 25 mol% O_2 and 25 mol% N_2. Permeate-side inlet: Ar.

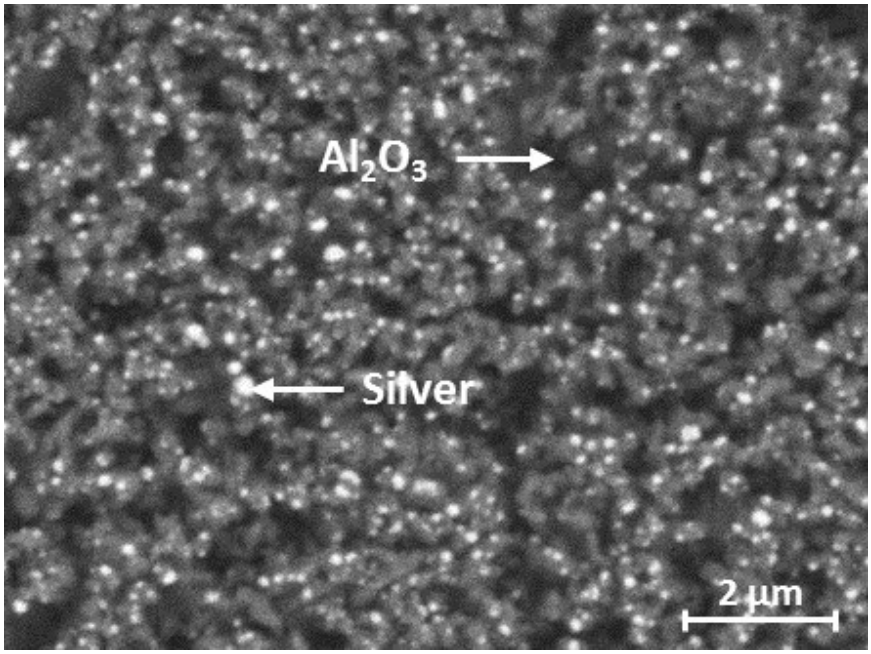

Fig. S11: Dry impregnation of Ag onto an Al_2O_3 pellet. SEM image of the feed side of a Ag dry-impregnated Al_2O_3 pellet, showing Ag nanoparticles dispersed across the surface.

Fig. S12: Ag sealant migration in dual-phase membranes. Al_2O_3 pellet membranes with 0 mol% Ag doping operated at 650 °C shows evidence of Ag dendrites within the cross-section of the membrane. Feed-side inlet: 50 mol% CO_2, 25 mol% O_2 and 25 mol% N_2. Permeate-side inlet: Ar.

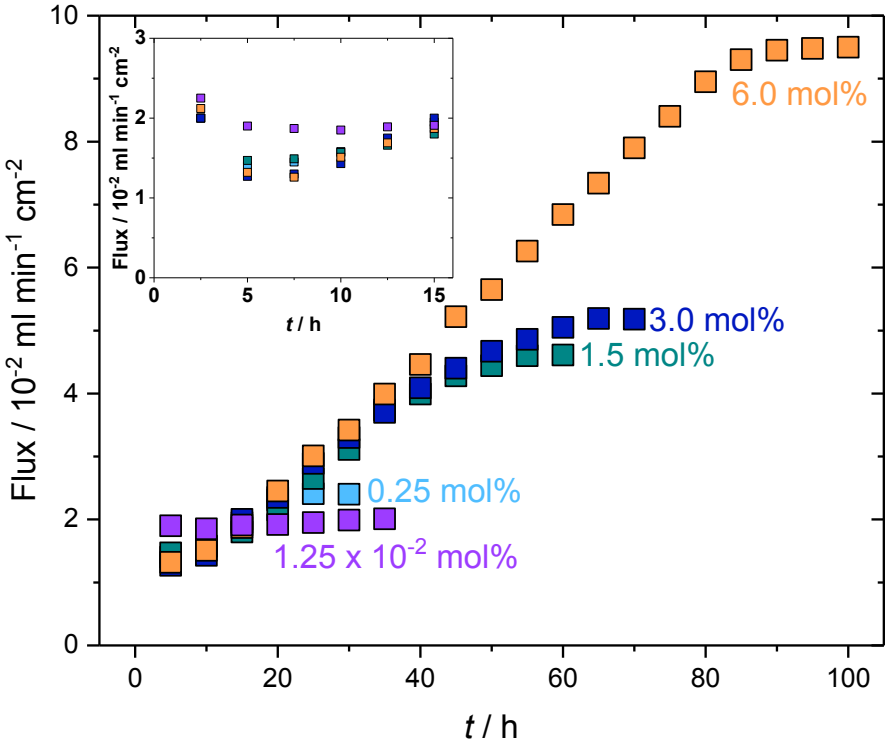

Fig. S13: Evolution towards stable flux in Ag-loaded pellet membranes. Al_2O_3 pellet membranes loaded with different mole fractions of Ag all demonstrated a constant low-flux region before 10 hours of permeation at 650 °C. Feed-side inlet: 50 mol% CO_2, 25 mol% O_2 and 25 mol% N_2. Permeate-side inlet: Ar.

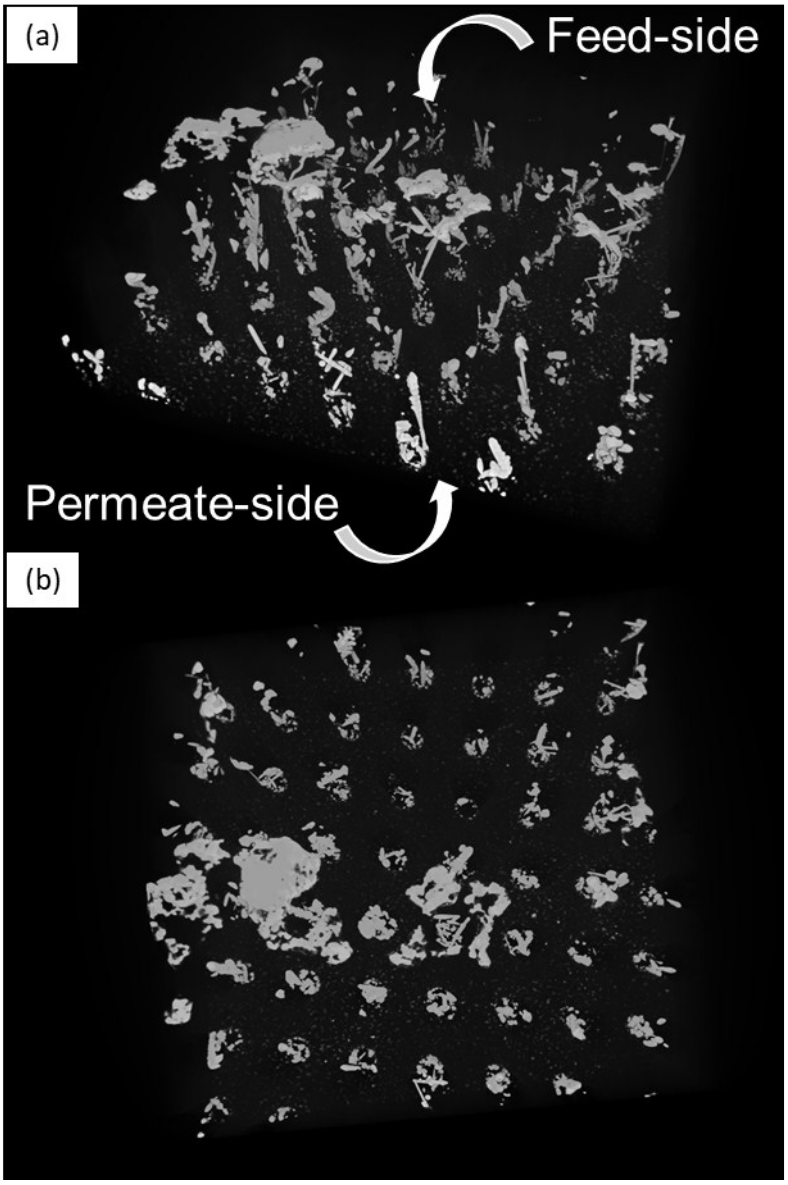

Fig. S14: 3D reconstruction of Ag within parallel-pores following a permeation experiment with Ag-loaded carbonates. (a) Perspective view, (b) plan view (feed side), both with the Al_2O_3 support removed in post-processing. The parallel-pore membrane was operated at 650 °C. Feed-side inlet: 50 mol% CO_2, 25 mol% O_2 and 25 mol% N_2. Permeate-side inlet: Ar.

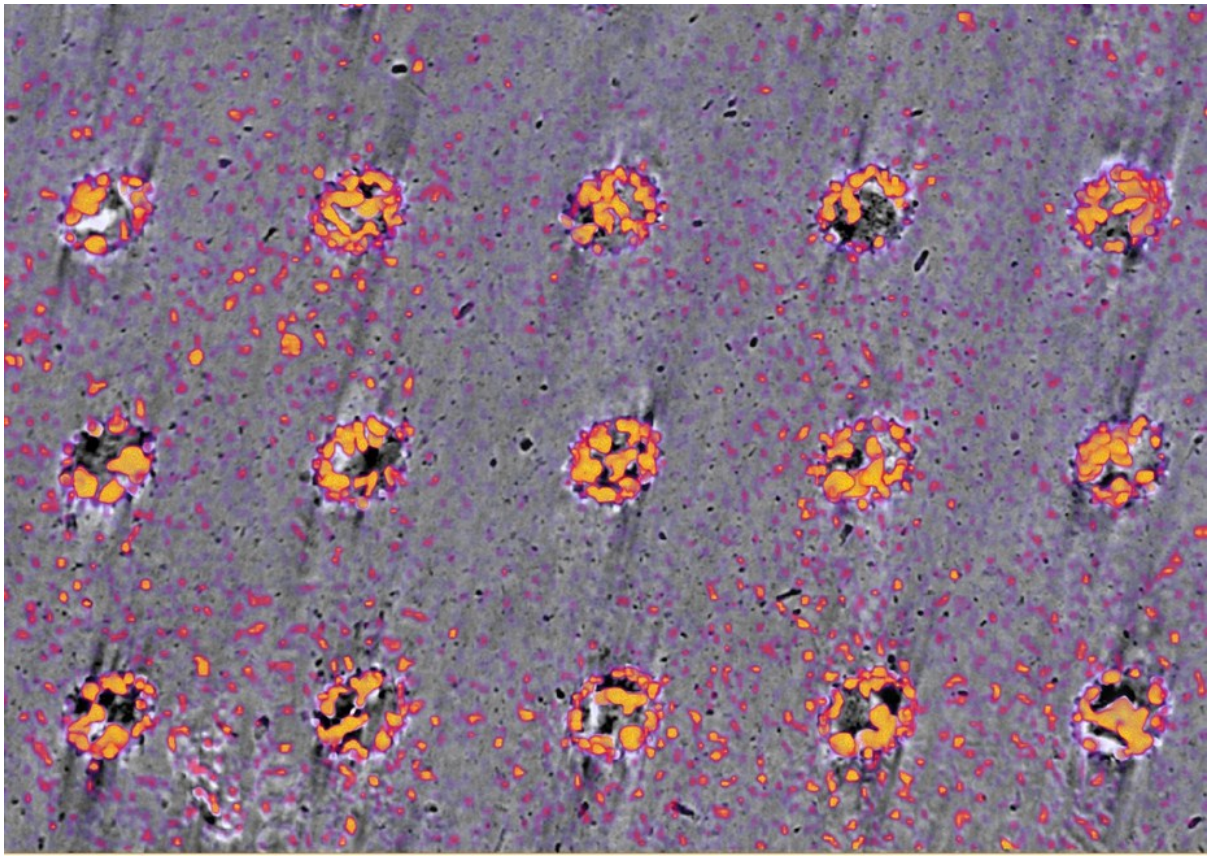

Fig. S15: Ag attachment to parallel-pore walls. Ag (orange) can be observed attached to the pore walls of the laser-drilled Al_2O_3 support. Clustering of Ag towards the middle of the pore is a result of the conical pore shape (150 µm Ø at the near surface, 75 µm Ø at the far surface).

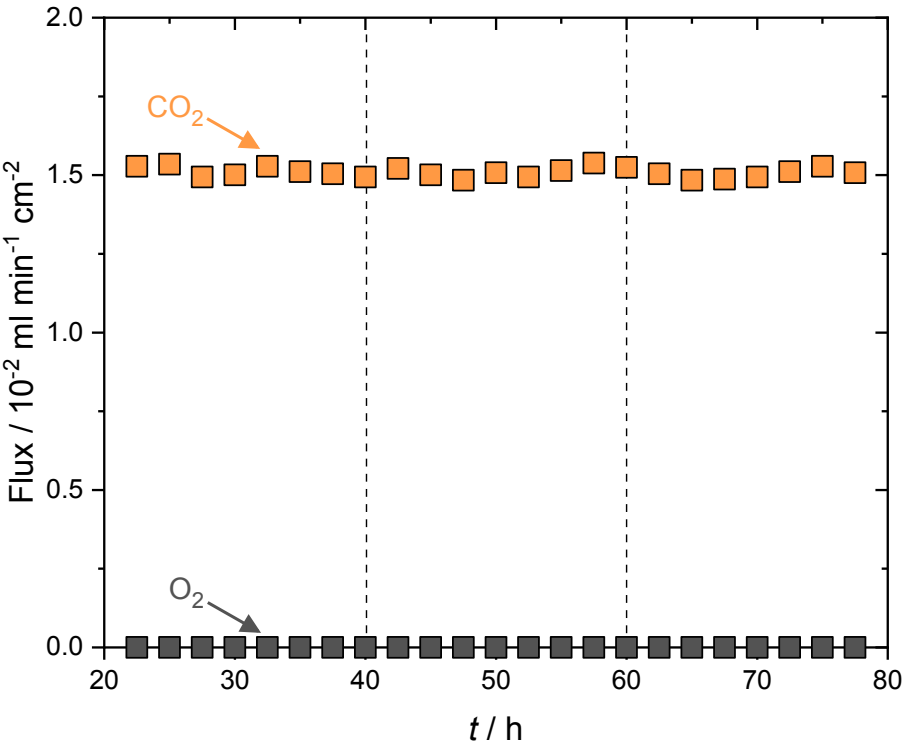

Fig. S16: Undoped parallel-pore membrane control experiment. CO_2 and O_2 flux at 650 °C in the parallel-pore membrane without the addition of Ag. During 20 – 40 h and 60 – 80 h the membrane feed-side inlet was 50 mol% CO_2, 25 mol% O_2 and 25 mol% N_2. During 40 – 60 h the membrane feed-side inlet was 50 mol% CO_2 and 50 mol% N_2. The permeate-side inlet was Ar throughout. Note that the CO_2 flux is almost two orders of magnitude lower than the parallel-pore Ag membrane in Fig. 6c.

References:

1 S. Frangini and A. Masi, *Int. J. Hydrogen Energy*, 2016, **41**, 18739–18746.

2 S. N. Paglieri and J. D. Way, *Sep. Purif. Methods*, 2002, **31**, 1–169.

3 P. P. Mardilovich, Y. She, Y. H. Ma and M.-H. Rei, *Separations*, 1998, **44**, 310–322.